Desalination and Water Treatment
www.deswater.com

doi: 10.5004/dwt.2018.21847

108 (2018) 97–105
March

Mechanism and performance of preparation of compositional sewage sludge and corn straw-derived activated carbon with KOH

Fan Zeng, Xiaofeng Liao, Li Liao, Hui Hu*

School of Environmental Science and Engineering, HuaZhong University of Science and Technology, 1037 Luoyu Road, Wu Han, China, CN 430074, Tel. +86 27 87792401; emails: huihu822@sina.com (H. Hu), fanfuzi3@163.com (F. Zeng), 575784633@qq.com (X. Liao), liaoli@hust.edu.cn (L. Liao)

Received 21 July 2017; Accepted 22 December 2017

ABSTRACT

Sewage sludge and corn straw-derived activated carbon (AC) were prepared by chemical activation with KOH and pyrolyzed in nitrogen atmosphere, then the effects of KOH dosage on the characteristics of AC were investigated. Thermal properties of materials were analyzed, and it was found that KOH facilitates the earlier decomposition of organics and promotes the pyrolysis process of the substances. Parameters such as specific surface area and pore size distribution of AC were studied. AC372 has the highest microporosity of 0.590, AC374 has the smallest average pore size of 3.657 nm, and AC376 has the highest S_{BET} value of 689.624 m^2/g. These indicate that the right amount of KOH (the mass ratio of sewage sludge, corn straw and KOH was 3:7:2) can promote the formation of micropores in AC, but an excessive KOH would etch or even block the original pore structure. The results of the Boehm titration and infrared spectroscopy analysis showed that the KOH activation did not only increase the number of basic groups on the surface of AC but also reduce the number of acidic groups. KOH, K_2CO_3, K_2O and other substances were detected in pyrolysis products by the XRD analysis. Thus indicates that H_2, CO, CO_2, K_2O and K_2CO_3 may be produced in the process of KOH activation.

Keywords: Sewage sludge; Corn straw; Activated carbon; KOH activation; Mechanism

1. Introduction

Containing a large amount of organic material (about 50%–70%), sewage sludge (SS) has the objective conditions of preparing the activated carbon. Using appropriate methods to prepare activated carbon (AC) by SS is not only an effective way of using carbon resources in sludge but also a solution to the sludge pollution. However, the high moisture and quartz sand contents in SS have negative effects; they led to a low yield and underdeveloped pore structure for AC, which cannot fulfill the wide range of industrial application standards. In order to prepare high-quality sludge-based activated carbon (SAC), the researchers added biomass waste such as straw [1], agricultural waste [2], bagasse wastes [3], peanut hull [4] and other auxiliary materials with high carbon content to improve the carbon content in raw materials. In addition, the use of highly efficient activator was another method to improve the yield and the quality of AC.

The common activation methods for the preparation of AC include physical activation and chemical activation. The physical activation method mainly uses water vapor [5,6], carbon dioxide [7,8] and other inert gas as an activator to prepare porous microcrystalline structure materials. However, the AC prepared by the physical activation method has a relatively low specific surface area and high ash content [9]. The chemical activation method mainly uses the chemical reagents to etch the organic matter in raw materials, thus establishing a developed pore structure in AC. Compared with the physical activation method, the chemical activation method has the advantages of short production cycle, high product yield, and the activator is recyclable. Chemical activation has been successfully applied to the production of ACs using various chemical reagents, that is, KOH [7],

* Corresponding author.

$ZnCl_2$ [10–14], H_2SO_4 [15–17] and H_3PO_4 [18]. Moreover, the chemical activation with hydroxides has been shown to be of great interest for the production of ACs with a highly microporous structure. Therefore, as the most ordinary alkaline substance, KOH has been used as activator in lots of studies related to the preparation of activated carbons by chemical activation. Monsalvo et al. [19] compared KOH, CO_2 and air as different activators during the preparation of sludge-based AC, and found that the activation with KOH gives the AC a much higher development of porosity. Hunsom and Autthanit [20] compared the activation effects of H_3PO_4, K_2CO_3 and KOH on the preparation of sludge-based AC, and found that KOH was the best. Lin et al. [21] prepared the sludge-based ACs with KOH, $ZnCl_2$ and H_3PO_4 as activators, the results showed that KOH had the best activation effect that can result in the highest specific surface area of AC.

The basic activator can react directly with the carbon atoms in the organic material, and form water vapor and small molecule hydrocarbons to escape, thereby forming porous material with developed porous structure and huge specific surface area [22]. Lillo-Ródenas et al. [23] studied the activation mechanism of the alkaline activator during the preparation of AC, the results show that the final product of KOH activation is K_2CO_3, H_2 and a small amount of Kang et al. [24] did not found the generation of K in the final product, but he found a small amount of CO_2 instead; furthermore, they also found that part of the atomic layer which formed under high temperature conditions could increase the internal pore structure of AC. Recently, some other researchers believe that the final product of KOH activation consists of not only K_2CO_3, H_2 and CO_2 but also K and K_2O [25,26].

By those methods, the powdery or granular AC which have abundant pore structures and high surface area are chosen as the adsorption materials, and using its physical and/or chemical adsorption characteristics to achieve the purpose of removing pollutants such as gaseous or liquid. Lu et al. [27] prepared AC with the mixture of cotton shells and SS, and he found that the mixture had better adsorption effects on methylene blue and Cu^{2+}. Wang et al. [28] used the AC prepared with the same materials to remove the dye pollution in waste water, and found that the removal rate was up to 99.7%. At present, there are many publications of the application studies of SAC related to the purification of phosphorus-containing wastewater [29,30], treatment of waste metal containing cadmium and lead [31,32], removal of COD from landfill leachate [33,34], and so on [35–37]. Some other researchers studied the application related to the exhaust gas purification research. The results obtained by a research team at the City University of New York have shown the potential of SAC as desulfurizers [38–43]. The team prepared AC by sludge obtained from municipal and industrial. The results show that SAC has a higher purification efficiency for H_2S, which is due to the rich pore structure and surface acid–base groups [44–46]. Therefore, the applications of SAC in pollutant treatment do not only achieve waste recycling purpose but also greatly reduce the cost of industrial applications.

According to the China's Yearbook data, the annual production of SS (with moisture content about 80%) is 30 to 40 million tons, and it is growing at the rate of 15% to 18% annually. Meanwhile, the annual production of crop straw is about 6.5×10^8 t. Based on these facts, proceed with the study of prepared AC by SS and straw has a wide range of applications. In this study, sludge-straw based AC was prepared by SS and corn straw (CS) with KOH activation, and the AC samples were characterized by various methods, such as TG–DTG, XRD, SEM, Fourier transform infrared spectroscopy (FT-IR) and so on. The effects of the amount of KOH on the specific surface area, pore structure, surface morphology and surface functional groups of AC were investigated, and the activation mechanism of KOH was derived. The proposed method can be expanded to the municipal solid waste recycling programs and renewable energy plans. Thus, the study of prepared AC by SS and CS as a carbon-based dry adsorbent agent could obtain huge social, economical and environmental benefits.

2. Materials and methods

2.1. Materials

The SS used in this study was dewatered activated sludge from a dehydration workshop of some municipal sewage treatment plants in Wuhan. The CS was obtained from the rural area of Henan Province, which is the largest agricultural province in China. The high purity nitrogen was produced by Wuhan Minghui Gas Technology Company with a purity of 99.999%. All chemicals used in this study were of analytical grade.

At the beginning, SS and corn stalks are naturally dried, then being dried at 105°C in the electro-thermostatic blast oven for 48 h. After a thorough drying, the mixture was crushed and an appropriate amount of samples were taken for the physicochemical characteristics analysis. The industrial and elemental analysis of the raw materials is shown in Table 1.

As can be seen from Table 1, the fixed carbon contents in CS and SS is 14.18 wt% and 5.18 wt%, respectively, which will be the source of carbon for ACs. In addition, the C element content in CS is 44.75 wt%, whereas the value in SS is only 20.00 wt%. Therefore, the two kinds of materials mentioned above mixed by certain conditions can obtain a mixture with moderate carbon content, which can be used for AC preparation.

Table 1
Physicochemical characteristics of raw materials

Raw	Proximate analysis (dry basis, wt%)				Ultimate (wt%)				
	Moisture	Volatiles	Ash	Fixed carbon	C	H	O	N	S
SS	2.96	36.72	55.14	5.18	20.00	3.65	19.65	3.32	3.19
CS	3.24	80.02	2.56	14.18	44.75	5.88	44.86	0.44	1.57

2.2. Preparation of the AC

Step 1: the SS and CS were dried to constant weight, crushed and sieved to less than 0.5 mm. Step 2: the SS and CS were mixed in a certain proportion as raw materials, and impregnated it with 2 g/L KOH solution for 6 h, then dried at 105°C in electro-thermostatic blast oven for 24 h. Step 3: the dried impregnated samples were then subjected to a pyrolysis process at 750°C for 60 min under a nitrogen flow of 100 mL/min, in a stainless steel tank (165 mm × 50 mm × 40 mm, ID) placed in a controlled atmosphere box furnaces (QXR1200-30, manufactured by Shanghai Qian Tong Technology Co., Ltd., China) at a heating rate of 10°C/min. After the completion of pyrolysis process, the furnaces were cooled to room temperature under a nitrogen atmosphere. Step 4: the carbonized samples were washed with 3 M HCl solution for 30 min to remove impurities and ash. Then they were continuously washed with hot distilled water (80°C) until the pH of the filtrate reaching about 7. Step 5: the washed samples were dried at 105°C to a constant weight to get different AC samples, and being named them with AC_i. Each experiment was carried out in triplicate.

The preliminary results of our research group showed that the optimal dry mass ratio for SS/CS was 3:7, with which the best AC samples were obtained [14,47]. Thus, this study mixed the SS and CS with a fixed ratio of W_{SS}:W_{CS} (3:7). However, the amount of activator KOH was adjusted to prepare six kinds of ACs with the mix ratio (W_{SS}:W_{CS}:W_{KOH}) of 3:7:0, 3:7:1, 3:7:2, 3:7:4, 3:7:6 and 3:7:10, and named as AC370, AC371, AC372, AC374, AC376 and AC3710, respectively.

2.3. Characterization of the samples

The weight loss behavior of raw materials was carried out with a Diamond TG/DTA Instrument (PerkinElmer Instruments, Germany). The heating rate was 10°C/min in a N_2 atmosphere with a 100 mL/min flow rate, and the samples were heated up to 750°C. The physical parameters of AC samples, such as adsorption/desorption characteristics, surface area and pore volume, were analyzed using an automatic specific surface area and porosity analyzer (JW-BK122W, JWGB Ltd., China). The crystallographic microstructure of AC samples was analyzed using an X-ray diffractometer (XRD) (X'Pert PRO, PANalytical B.V., Netherlands), which was carried out at a scanning diffraction angle of 10°–80°. The structures and functional groups of the samples were analyzed by FT-IR (Bruker VERTEX 70, Germany) and Boehm titration method. The surface microstructure of the AC samples was examined using a scanning electronic microscopy (SEM) (Nova NanoSEM 450, FEI, Netherlands).

3. Results and discussion

3.1. Effects of KOH amount on thermal properties of raw materials

The thermo gravimetric analysis of the SS, CS and several KOH-impregnated mixed materials was carried out, respectively. TG (a) and DTG (b) curves of SS, CS and their compound mixed with KOH are shown in Fig. 1.

According to previous studies on pyrolysis behaviors, the entire pyrolysis process profile could be divided into three stages/phases as dehydration phase, devolatilization and combustion phase, and char combustion phase, respectively [48,49]. As can be seen from the TG–DTG curves in Fig. 1(a1), the weight loss of SS can be divided into three stages. Stage one, the amount of weight loss in 40~150°C is small, which due to the loss of moisture present and the bound water in SS, it can be called dehydration phase. However, the weight loss is not obvious as the raw materials were processed through a drying treatment. The second weight loss stage occurs at 150~400°C and the phenomenon is more obvious, and it can be called as devolatilization phase. There are two peaks of DTG curve occurring at 270°C and 310°C. This dramatic weight loss is due to the removal of volatile matter such as lipids, sugars, proteins in SS and the value of weight loss was 29.83%. The third weight loss stage occurring at the temperature within 400°C–600°C is associated with the decomposition of residual organic and inorganic salts, which can be called as char combustion phase, and resulting in less weight loss.

Similarly, the weight loss of CS also appears in three stages. The same as mentioned above, the dehydration phase ranged from 40°C to 150°C, and as there was higher moisture in CS, the weight loss was bigger. Additionally, the value of weight loss in the devolatilization phase (occurring at 150°C–400°C) is more dramatic, up to 70.43%, and the highest weight loss rate appears at 340°C. This dramatic phenomenon of weight loss is due to the pyrolysis emissions of cellulose, hemicellulose and other organic matter in CS [50]. In addition, the TG curve of the CS falls greater, which may attribute to the more organic constituents and the less ash content. And the third weight loss step of char combustion phase occurred in the range of 400°C–600°C, and has a weight loss of 4.53%. However, the cause of weight loss has changed, which is due to the decomposition of the lignin [51,52].

As shown in Fig. 1(a3), the TG–DTG curves of the inactivated mixture (W_{SS}:W_{CS}:W_{KOH} = 3:7:0) is similar to that of the CS which is the major ingredient in the mixture. The value of weight loss in the devolatilization phase which occurs at 150°C–400°C is up to 59.07%, and the highest peak appears at 340°C, too. However, the TG–DTG curves of the mixed materials which were impregnated by KOH solution changed significantly. As shown in Fig. 1(a4), the TG–DTG curves of the activated mixture (W_{SS}:W_{CS}:W_{KOH} = 3:7:2) also presents in three stages, however, the dramatic weight loss in the devolatilization phase which occurs at 150°C–400°C have an earlier sharp peak of DTG curve occurring at 250°C. As the increase of KOH dosage, which is shown in Fig. 1(a5), the weight loss of the activated mixture (W_{SS}:W_{CS}:W_{KOH} = 3:7:10) no longer presents the same three intervals, the highest peak of weight loss appears earlier. The devolatilization phase occurs from 90°C to 400°C, and two DTG peak have been observed both in devolatilization phase and char combustion phase. Additionally, even in the range of 600°C–750°C, weight loss phenomenon appears, which may be due to the decomposition of the refractory substances. As shown in Fig. 1(b), the DTG curves of two activated mixtures have weight loss peaks at a lower temperature, which means the decomposition of volatile matter in biomass can be started at relatively low temperature. These phenomena indicate that the presence of KOH facilitates the earlier decomposition of organic matter such as cellulosic substances, and promotes the pyrolysis of refractory substances in the raw materials.

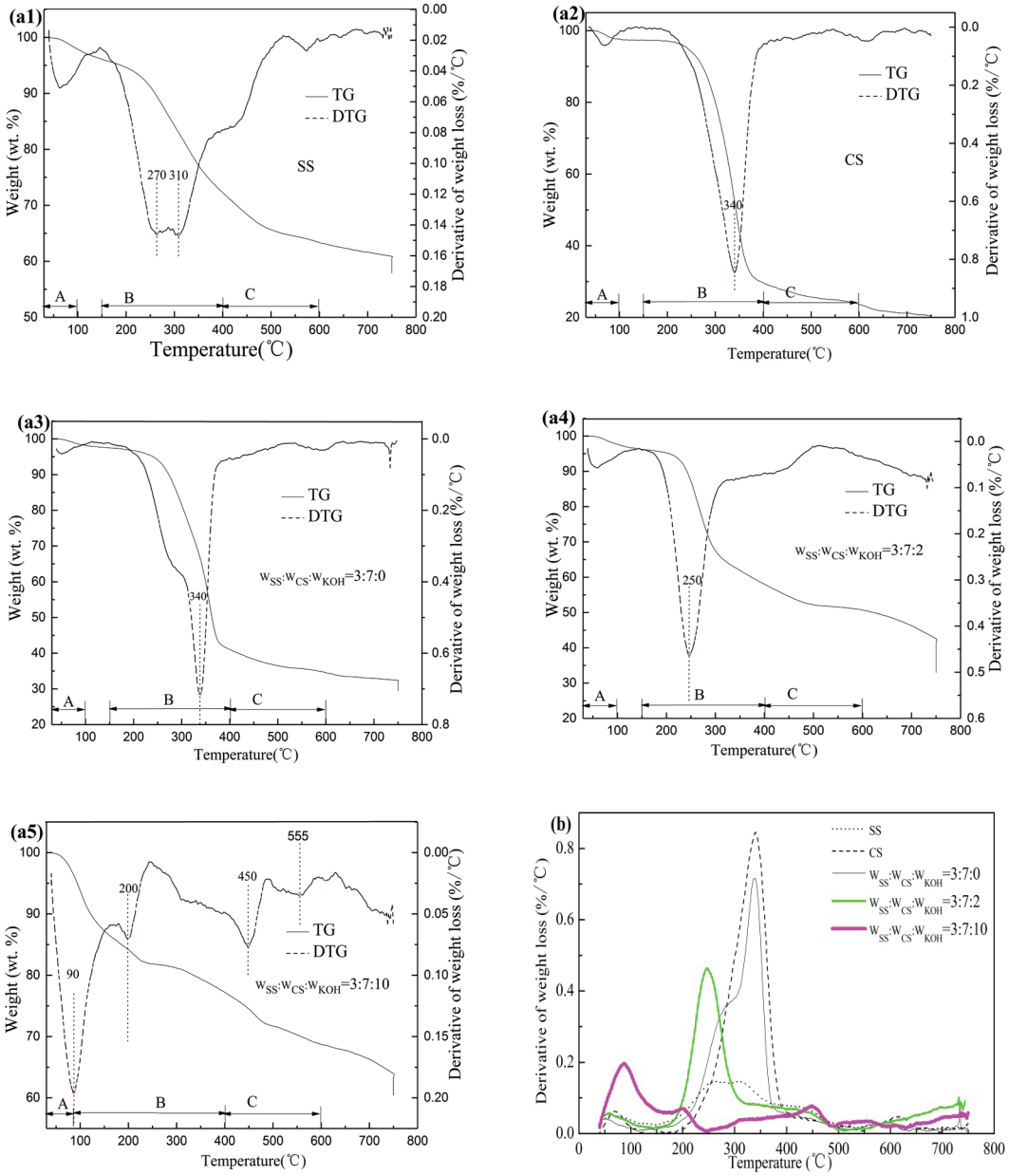

Fig. 1. TG and DTG curves of SS(a1), CS(a2) and KOH-impregnated mixed materials (precursor of AC370(a3), precursor of AC372(a4), precursor of AC3710(a5), DTG curves of all samples(b)).

3.2. Effects of KOH amount on pore characteristic

As known, the adsorption performance of AC is related to the BET surface area and the pore structure. The N_2 adsorption/desorption isotherms and pore size distributions can reflect the pore structure, the specific surface area and the pore type of the materials, which is an important method to characterize the pore structure of AC. Fig. 2 shows the N_2 adsorption/desorption isotherms of the AC samples, and Table 1 shows the pore structure parameters of each sample.

As shown in Fig. 2, according to the classification of IUPAC, the nitrogen adsorption isotherms of six kinds of AC samples have evident type IV isotherms, and there are hysteresis loops can be observed in the adsorption/desorption isotherms, indicating the existence of mesoporous structures in samples [53]. However, as the amount of KOH increases, the hysteresis loop gradually changed from H4 (Fig. 2(a)) to H3 (Fig. 2(b)), indicating that the slit-like pores in the AC are gradually destroyed and changed into plate-like particles, then these plate-like particles are combined and form new pores [53]. These changes led to the nitrogen adsorption capacity of AC samples become larger when the relative pressure is low, and this phenomenon means the increase of micropores content in AC [54].

As can be seen from Table 2, the characteristic parameters of AC samples prepared by the mixed materials impregnated by KOH solution are much better than those prepared by the inactivated mixture. Moreover, as the amount

of KOH increased appropriately, the quality of AC samples improved. The S_{BET} values showed that the addition of KOH results in a great increase of the surface area of the AC samples, and as the amount of KOH increased, the S_{BET} values of the samples presents a tendency of increased first and then decreased. AC376 has the highest S_{BET} value of 689.624 m^2/g, which is nine times higher than that of AC370. This is related to the improvement of micropores in AC samples. AC376 also has the highest V_{total} and V_{micro} value, which are 0.737 and 0.372 cm^3/g, respectively. However, though the microporosity (defined as V_{micro}/V_{total}) appeared the same tendency of increased first and then decreased with the amount of KOH increased, the highest microporosity was obtained by AC372, which is 0.590.

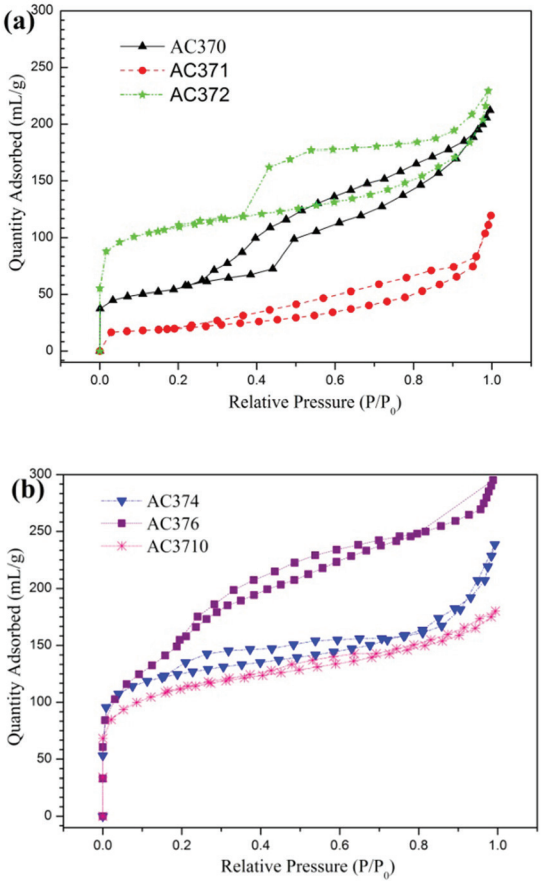

Fig. 2. The N_2 adsorption/desorption isotherms of ACs with different mixture/KOH ratios (a) AC370, AC371 and AC372, (b) AC374, AC376 and AC3710.

Specifically, the D_{ave} values of the samples appeared with the contrary tendency of decreasing first and then increasing as the amount of KOH increased, and AC374 has the smallest average pore size of 3.657, indicative of its mesoporous character. The data above indicate that the characteristic parameters of the AC sample did not continue to improve with the amount of KOH increased. Hence, before pyrolysis, impregnating the mixed materials with the right amount of activator KOH can promote the formation of micropores in AC samples, but as KOH is used in excessive amount, its effectiveness in expansion of pore is more obvious. It is assumed that excessive KOH will etch the pore walls between the micropores in AC, the walls would be thinned or even burned through, then the micropores were expanded to mesopores or even macropores; additionally, before the excessive KOH at the active site diffused into the inside of the carbon particles, part of them had undergone chemical reaction with surface groups from the carbon skeleton, which will led to a serious burnout and restrict the formation and development of micropores [55].

For a more intuitive understanding of the pore structure distribution of AC, three samples were selected for SEM, and the results are shown in Fig. 3.

It can be seen that different surface morphologies were observed in the three AC samples studied. Fig. 3(a) shows the surface morphology of AC370, which was prepared by an inactivated mixture. It shows that AC370 has a smooth uniform surface with layered large-diameter pores and craters, and presents an obvious cross-link structure. AC371 displays an irregular and uneven surface, the chain-like transverse bonding was destroyed, and new small pores were formed in the large agglomerated pore structure. Fig. 3(c) shows the surface morphology of AC3710, which was impregnated with excessive KOH. It can be seen that the micellar pore structure was reduced and a large amount of uniform flaky material appeared on the surface, which may be the residual potassium salt. The comprehensive analysis shows that the AC preparation with the same ratio of raw materials, adding an appropriate amount of KOH is beneficial to the formation of the pore structure in AC, but an excessive KOH will etch the original pore structure, and even block part of the pore structure. The phenomenon above verified the pore size distribution of the AC sample.

Table 2
Pore structure parameters of AC samples

Adsorbent	S_{BET} (m^2/g)	S_{micro} (m^2/g)	D_{ave} (nm)	V_{total} (cm^3/g)	V_{micro} (cm^3/g)	V_{micro}/V_{total}
AC370	68.920	0.707	7.563	0.133	0.001	0.008
AC371	214.813	159.854	4.493	0.328	0.113	0.345
AC372	369.271	293.931	4.000	0.256	0.151	0.590
AC374	403.495	302.072	3.657	0.269	0.158	0.587
AC376	689.624	283.164	3.965	0.737	0.372	0.505
AC3710	420.545	280.786	4.432	0.316	0.154	0.487

S_{BET}, BET surface area; S_{micro}, micropores surface area; D_{ave}, average pore diameter; V_{total}, total pore volume; V_{micro}, micropores volume.

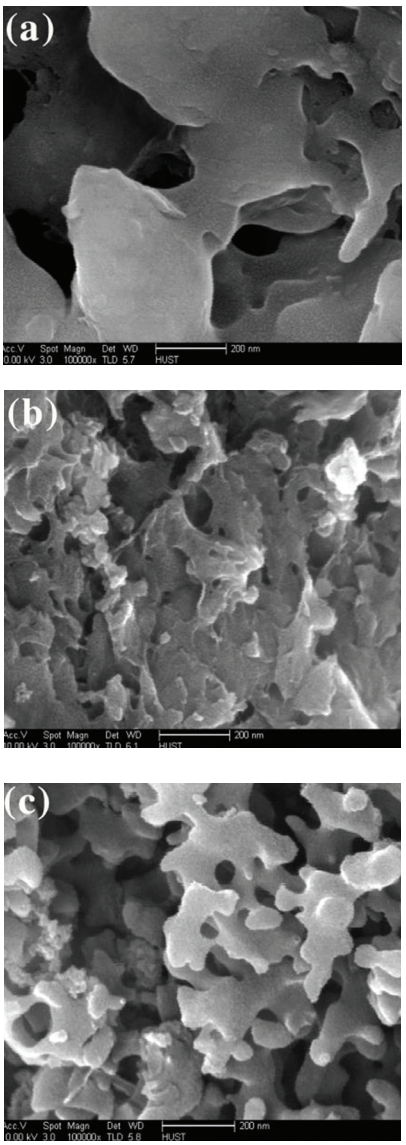

Fig. 3. SEM photographs of AC370 (a), AC372 (b) and AC3710 (c).

3.3. Effects of KOH amount on surface chemistry

The adsorption properties of AC are determined not only by their pore structure but also related to the type and number of surface functional groups on the surface [56]. The Boehm titration results showed that KOH activation not only increases the number of basic groups on the surface of AC but also reduces the number of acidic groups. It is reported that the removal of acidic groups can further develop the pore structure of AC [57]. In order to give a further identification of the functional groups on the surface of the AC samples, AC370, AC372, AC374 and AC3710, were selected for infrared spectroscopy (FT-IR) analysis. The results are shown in Fig. 4.

As shown in Fig. 4, the FT-IR spectra of the AC samples which were prepared by the mixed materials impregnated with KOH solution were similar, but they were obviously different from the spectra of AC370. The changes in the type and content of the functional groups on the surface of the

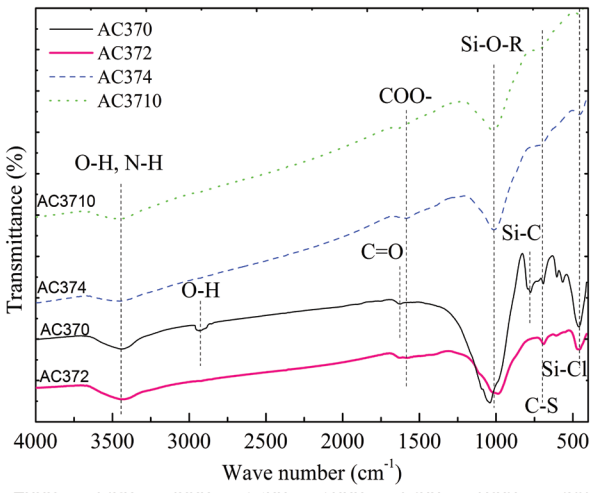

Fig. 4. FT-IR spectra of the AC samples.

sample may be caused from the erosion of the carbon skeleton by the activator under the high temperature. The broad and flat band at 3,450 cm^{-1} can be assigned to compounds with hydroxyl group (O–H) and/or nitrogen-containing surface group (N–H). The strong absorption band observed at 990 to 1,050 cm^{-1} can be assigned to Si–O–R (where R = Si, Al, Fe, Ca and Zn). The two bands above can be visible for all four samples, which may be related to the main raw materials of SS and CS.

In the spectra of AC370, there were stretching vibration peak of O–H (2,920 cm^{-1}) and associating C=O (1,650 cm^{-1}), which not being observed in another three AC samples, they indicate that AC370 contains greater number of carboxylic acid compounds. However, a new carboxylate characteristic peak appeared at 1,590 cm^{-1} in the FT-IR spectra of another three AC samples. As reported, when the carboxylic acid reacts with the alkali to form carboxylate, the infrared spectrum has a great change; the original O–H, C=O stretching vibration characteristic peaks disappeared, while new asymmetric stretching vibrations of COO^- (1,610–1,550 cm^{-1}) appeared [58]. In addition, comparing the absorption peaks of the four samples, the Si–C stretching vibration (780 cm^{-1}) was only being observed in AC370, indicating that the Si–C bond can be completely destroyed by the activator at high temperatures, thus providing conditions for the formation of the pore structure. The result of FT-IR analysis confirmed the conclusion by the Boehm titration study.

3.4. Effects of KOH on pyrolysis products

The pyrolysis products were analyzed in order to validate the effectiveness of the activator KOH during the preparation of AC samples. After the pyrolysis reaction is completed, in reaction tank of the activated mixture, some by-products of dark white substance were observed on the surface of the unwashed pyrolysis products, and these by-products increased as the addition amount of KOH increased. However, the by-products did not appear in the reaction tank of the inactivated mixture. The detection of these by-products shows that, these unknown substances can react violently with water, accompanied by a large amount

of bubbles generated, and the solution was alkaline after the reaction. In addition, the unknown substances can also react with the acid, and release a large amount of gases which can make clear lime water turbid. As the phenomenon described above, it can be inferred that the by-product may contain K, K_2O and K_2CO_3. In order to further verify the inference mentioned above, AC372 and AC3710 were selected for XRD analysis, and choosing K_2CO_3 as a comparative substance. The result is shown in Fig. 5.

Silva et al. [59] examined the morphologies of the SS by pyrolysis at 750°C, and the XRD patterns showed the presence of SiO_2 and $CaCO_3$. The peaks of SiO_2 were mainly observed at 2θ of 21° and 26°, whereas the peaks of $CaCO_3$ at 2θ of 37° [59]. This may be due to the raw materials obtained from the industrial laundry. Angeles Lillo-Ródenas et al. [60] studied the changes in the mineral matter composition and those accompanying during the KOH activation process of the SS by XRD, besides the SiO_2 at 2θ of 26°, they also observed many compounds containing potassium, such as potassium hydroxide, potassium carbonate, potassium hydroxide hydrate, potassium oxide and so on.

As shown in Fig. 5, the spectra of K_2CO_3 substance does not show any obvious X-ray diffraction peak, only several weak peaks can be observed, which can be assigned to the K_2CO_3 and K_2O [60]. However, the X-ray diffraction peak of AC372 and AC3710 are more obvious, there are several obvious X-ray diffraction peaks. Tang et al. [61] believed some minerals can be reorganized into different crystal structures, according to the conditions of temperature. The distinct peaks of SiO_2 were observed in the XRD patterns of AC372 and AC3710. Additionally, another main diffraction peaks can be assigned to KOH, KOH-hydrate, K_2CO_3 and K_2O [23,62].

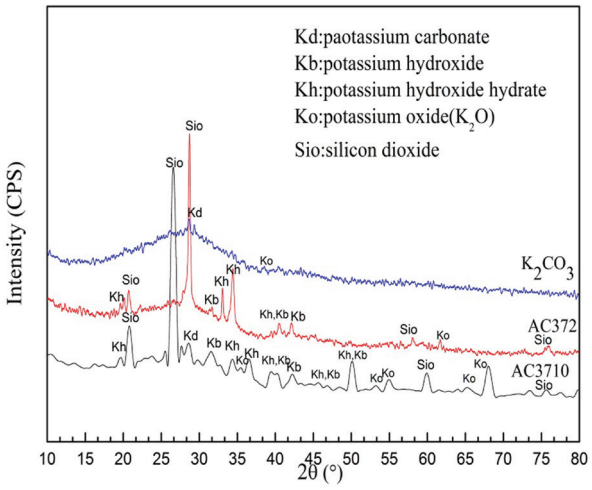

Fig. 5. XRD spectra of different activated carbons and K_2CO_3.

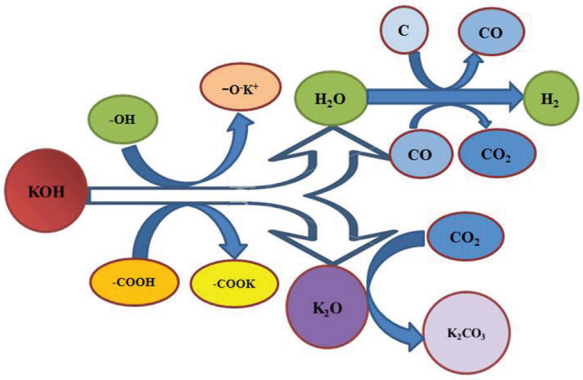

Fig. 6. Reaction flow chart of KOH activation.

3.5. Activation mechanism of KOH

Based on the results above, we can speculate the reaction flow chart of KOH activation in the preparation of activated carbon, which is shown in Fig. 6. In the nitrogen atmosphere and at a sufficient temperature conditions, activator KOH reacts with the surface oxygen-containing groups such as –OH and –COOH in the raw materials, which led to the generation of the active components such as $–O^-K^+$ and –COOK. These active components are introduced onto the surface of the reaction mass where they can be better contacted. This process lays the foundation for pyrolysis. The reaction of this stage can be expressed as Eqs. (1) and (2) below:

$$KOH + –OH \rightarrow –O^-K^+ + H_2O \quad (1)$$

$$KOH + –COOH \rightarrow –COOK + H_2O \quad (2)$$

As the reaction temperature continues to rise, KOH turns into molten state, and its own bases are responsible for its dehydration reaction. The reaction of this stage can be expressed as Eqs. (3) below:

$$2KOH \rightarrow K_2O + H_2O \quad (3)$$

In the meantime, the hydrogen atoms in the tar produced by the reaction of the organic matter are replaced by the partial $–O^-K^+$ groups, and a large amount of hydrogen atoms are released in the form of H_2, thereby suppressing the volatilization of the tar. Significantly, this process is also the key to increasing the yield of AC in the product. On the other hand, with the promotion of active components, the H_2O which was produced in the previous stage reacted with carbon element in volatile organic compounds, and produced other gases such as H_2, CO and CO_2. This results in the decomposition of the disordered cross-linked crystallites. In addition, another compound was generated during the process, which was K_2CO_3. As reported elsewhere [63,64], the likely reflects of the various elementary reactions can be outlined as Eqs. (4)–(6):

$$C + H_2O \rightarrow H_2 + CO \quad (4)$$

$$CO + H_2O \rightarrow H_2 + CO_2 \quad (5)$$

$$K_2O + CO_2 \rightarrow K_2CO_3 \quad (6)$$

On the whole, the use of activator KOH has a positive effect on pyrolysis and carbonization in the process of preparing AC with SS and CS. On the one hand, part of KOH participated in the pyrolysis reaction of the biomass substance in raw materials, which destroyed the structure of the macromolecular chains, and contributed to the formation of the carbon skeleton. On the other hand, KOH participated in the reaction and produced several small molecule gases. As these gases escaped, varieties of pore structure were formed, which was one of the main sources of AC pore structure.

4. Conclusions

KOH activator has a positive effect on improving the quality of activated carbon samples. With the increase in the amount of KOH, the S_{BET} values and the microporosity of the AC samples present a tendency of increasing first and then decreasing, the D_{ave} values have a contrary tendency. AC376 has the highest S_{BET} value of 689.624 m^2/g, AC372 has the highest microporosity of 0.590, which is nine times and 72.8 times higher than that of AC370, respectively. AC374 has the smallest average pore size of 3.657 nm.

The addition of KOH does not only increase the number of basic groups on the surface of AC but also reduce the number of acidic groups. The surface chemical groups of the AC prepared by inactivated mixture are dominated by the acidic groups, while in AC prepared by activated mixture they are dominated by the alkaline groups.

In all cases, KOH activation facilitates the earlier decomposition of the organic matters such as cellulosic substances, and promotes the pyrolysis of the refractory substances in the raw materials, and an appropriate amount of KOH can help achieving important porosity developments and promoting the formation of micropores. However, an excessive KOH will led to a serious burnout and restrict the formation and development of micropores, even once again crystallize into KOH or generate K_2CO_3 to block part of the original pore structure.

Acknowledgment

This work was supported by the National Key Technology R&D Program of China (NO. 2012BAC18B02).

References

[1] Y.L. Li, L.P. Li, J. Yin, W.J. Liang, J. Li, Optimization and preparation of sludge-based activated carbon by two-step pyrolysis and performance characterization, J. Beijing Univ. Technol., 39 (2013) 1887–1890.
[2] A.M. Abioye, F.N. Ani, Recent development in the production of activated carbon electrodes from agricultural waste biomass for super capacitors: a review, Renew. Sust. Energy Rev., 52 (2015) 1282–1293.
[3] H.B. Feng, H. Hu, H.W. Dong, Y. Xiao, Y.J. Cai, B.F. Lei, Y.L. Liu, M.T. Zheng, Hierarchical structured carbon derived from bagasse wastes: a simple and efficient synthesis route and its improved electrochemical properties for high-performance super capacitors, J. Power Sources, 302 (2016) 164–173.
[4] Y. Liu, Q. Chen, Z.R. Niu, X.X. Wang, X.H. Lei, K.Y. Yang, Preparation of peanut hull sludge-based activated carbon and application for oily wastewater treatment, Environ. Pollut. Control, 38 (2016) 43–47.
[5] S. Rio, L. Le Coq, C. Faur, P. Le Cloirec, Production of porous carbonaceous adsorbent from physical activation of sewage sludge: application to wastewater treatment, Water Sci. Technol., 53 (2006) 237–244.
[6] K.B. Fitzmorris, I.M. Lima, W.E. Marshall, R.S. Reimers, Anion and cat ion leaching or desorption from activated carbons from municipal sludge and poultry manure as affected by pH, Water Environ. Res., 78 (2006) 2324–2329.
[7] A. Ros, M.A. Lillo-Ródenas, E. Fuente, M.A. Montes-Morán, M.J. Martín, A. Linares-Solano, High surface area materials prepared from sewage sludge-based precursors, Chemosphere, 65 (2006) 132–140.
[8] J. Alvarez, G. Lopez, M. Amutio, M. Olazar, Preparation of adsorbents from sewage sludge pyrolytic char by carbon dioxide activation, Process Saf. Environ., 103 (2016) 76–86.
[9] K.M. Smith, G.D. Fowler, S. Pullket, N.J.D. Graham, Sewage sludge-based adsorbents: a review of their production, properties and use in water treatment applications, Water Res., 43 (2009) 2569–2594.
[10] N.R. Khalili, M. Campbell, G. Sandi, J. Golas, Production of micro-and mesoporous activated carbon from paper mill sludge: I. Effect of zinc chloride activation, Carbon, 38 (2000) 1905–1915.
[11] X.G. Chen, S. Jeyaseelan, N. Graham, Physical and chemical properties study of the activated carbon made from sewage sludge, Waste Manage., 22 (2002) 755–760.
[12] G. Sandí, N.R. Khalili, W. Lu, J. Prakash, Electrochemical performance of carbon materials derived from paper mill sludge, J. Power Sources, 119 (2003) 34–38.
[13] L.L. Yu, Q. Zhong, Preparation of adsorbents made from sewage sludges for adsorption of organic materials from wastewater, J. Hazard. Mater., 137 (2006) 359–366.
[14] Y. He, X.F. Liao, L. Liao, W. Shu, Low-cost adsorbent prepared from sewage sludge and corn stalk for the removal of COD in leachate, Environ. Sci. Pollut. Res., 21 (2014) 8157–8166.
[15] A. Bagreev, T.J. Bandosz, H_2S adsorption/oxidation on materials obtained using sulphuric acid activation of sewage sludge-derived fertilizer, J. Colloid Interface Sci., 252 (2002) 188–194.
[16] M. Martin, A. Artola, M. Balaguer, M. Rigola, Towards waste minimization in WWTP: activated carbon from biological sludge and its application in liquid phase adsorption, J. Chem. Technol. Biotechnol., 77 (2002) 825–833.
[17] M. Martin, A. Artola, M. Balaguer, M. Rigola, Activated carbons developed from surplus sewage sludge for the removal of dyes from dilute aqueous solutions, Chem. Eng. J., 94 (2003) 231–239.
[18] F.S. Zhang, J.O. Nriagu, H. Itoh, Mercury removal from water using activated carbons derived from organic sewage sludge, Water Res., 39 (2005) 389–395.
[19] V.M. Monsalvo, A.F. Mohedano, J.J. Rodriguez, Activated carbons from sewage sludge: Application to aqueous-phase adsorption of 4-chlorophenol, Desalination, 277 (2011) 377–382.
[20] M. Hunsom, C. Autthanit, Adsorptive purification of crude glycerol by sewage sludge-derived activated carbon prepared by chemical activation with H_3PO_4, K_2CO_3 and KOH, Chem. Eng. J., 229 (2013) 334–343.
[21] Q.H. Lin, H. Cheng, G.Y. Chen, Preparation and characterization of carbonaceous adsorbents from sewage sludge using a pilot-scale microwave heating equipment, J. Anal. Appl. Pyrol., 93 (2012) 113–119.
[22] A. Ahmadpour, D.D. Do, The preparation of activated carbon from macadamia nutshell by chemical activation, Carbon, 35 (1997) 1723–1732.
[23] M.A. Lillo-Ródenas, D. Cazorla-Amoro´s, A. Linares-Solano, Understanding chemical reactions between carbons and NaOH and KOH: an insight into the chemical activation mechanism, Carbon, 41 (2003) 267–275.
[24] H.Y. Kang, S.S. Park, Y.S. Rim, Preparation of activated carbon from paper mill sludge by KOH-activation, Korean J. Chem. Eng., 23 (2006) 948–953.
[25] J. Wang, S. Kaskel, KOH activation of carbon-based materials for energy storage, J. Mater. Chem., 22 (2012) 23710–23725.
[26] J. Zhang, J.M. Gao, Y. Chen, X.J. Jin, Preparation and characterization of the carbon purified from the walnut shells activated chemically with KOH, Results Phys., 7 (2017) 1628–1633.

[27] X.L. Lu, Preparation of Absorbent Using Sewage Sludge and Its Application on Wastewater Treatment, Wuhan University of Science and Technology, 2015.
[28] X.M. Wang, N.W. Zhu, B.K. Yin, Preparation of sludge-based activated carbon and its application in dye wastewater treatment, J. Hazard. Mater., 153 (2008) 22–27.
[29] D.C. Huang, H.S. Wang, Y.J. Zou, S. Xu, Y.J. Lai, J.Q. Yang, Adsorption of phosphorus from aqueous solution on activated stalk-carbon prepared under condition of atmosphere, Chin. J. Environ. Eng., 3 (2015) 1183–1188.
[30] R.H. Shao, P. Fang, Y.R. Lin, On the treatment of the phosphorus wastewater by using the sewage sludge-based activated carbon, J. Saf. Environ., 16 (2016) 267–273.
[31] P. Lodeiro, J.L. Barriada, R. Herrero, M.E. Sastre, The marine macroalga *Cystoseira baccata* as biosorbent for cadmium (II) and lead (II) removal: kinetic and equilibrium studies, Environ. Pollut., 142 (2006) 264–273.
[32] H.Y. Chen, Y.J. Yang, Z.J. Zhang, X.D. Tan, X. Xin, F.M. Liu, Effects of the preparation conditions of municipal sewage sludge bentonite absorbent on adsorption of Pb^{2+}, Chem. Res. Appl., 22 (2010) 800–804.
[33] Y.L. Chen, B.T. Li, Study on the advanced treatment of landfill leachate by activated carbon made from sewage sludge and straw, Environ. Pollut. Control, 2 (2014) 67–70,75.
[34] Y. He, W. Shu, X.F. Liao, T.Y. You, L. Liao, Preparation of sludge-stalk based activated carbon and its adsorption of COD in leachate, Chin. J. Environ. Eng., 9 (2015) 1663–1669.
[35] Y.B. Zhai, H.M. Chen, B.B. Xu, B.B. Xiang, C. Zhong, C.T. Li, G.M. Zeng, Influence of sewage sludge-based activated carbon and temperature on the liquefaction of sewage sludge: yield and composition of bio-oil, immobilization and risk assessment of heavy metals, Bioresour. Technol., 159 (2014) 72–79.
[36] J. Ábrego, J. Arauzo, J.L. Sánchez, A. Gonzalo, T. Cordero, J.R. Mirasol, Structural changes of sewage sludge char during fixed-bed pyrolysis, Ind. Eng. Chem. Res., 48 (2009) 3211–3221.
[37] H.M. Chen, Y.B. Zhai, B.B. Xu, B.B. Xiang, L. Zhu, L. Qiu, X.T. Liu, C.T. Li, G.M. Zeng, Characterization of bio-oil and biochar from high-temperature pyrolysis of sewage sludge, Environ. Technol., 36 (2014) 470–478.
[38] A. Bagreev, S. Bashkova, D.C. Locke, T.J. Bandosz, Sewage sludge-derived materials as efficient adsorbents for removal of hydrogen sulfide, Environ. Sci. Technol., 35 (2001) 1537–1543.
[39] A. Bagreev, J.A. Menendez, I. Dukhno, Y. Tarasenko, T.J. Bandosz, Bituminous coal-based activated carbons modified with nitrogen as adsorbents of hydrogen sulfide, Carbon, 42 (2004) 469–476.
[40] T.J. Bandosz, On the adsorption/oxidation of hydrogen sulfide on activated carbons at ambient temperatures, J. Colloid Interface Sci., 246 (2002) 1–20.
[41] T.J. Bandosz, K. Block, Municipal sludge-industrial sludge composite desulfurization adsorbents: synergy enhancing the catalytic properties, Environ. Sci. Technol., 40 (2006) 3378–3383.
[42] T.J. Bandosz, M. Seredych, Tobacco waste/industrial sludge based desulfurization adsorbents: effect of phase interactions during pyrolysis on surface activity, Environ. Sci. Technol., 41 (2007) 3715–3721.
[43] S. Bashkova, F.S. Baker, X.X. Wu, T.R. Armstrong, V. Schwartz, Activated carbon catalyst for selective oxidation of hydrogen sulphide: on the influence of pore structure, surface characteristics, and catalytically-active nitrogen, Carbon, 45 (2007) 1354–1363.
[44] R. Yan, T. Chin, Y.L. Ng, H.Q. Duan, D.T. Liang, J.H. Tay, Influence of surface properties on the mechanism of H_2S removal by alkaline activated carbons, Environ. Sci. Technol., 38 (2004) 316–323.
[45] S. Pipatmanomai, S. Kaewluan, T. Vitidsant, Economic assessment of biogas-to-electricity generation system with H_2S removal by activated carbon in small pig farm, Appl. Energy, 86 (2009) 669–674.
[46] Q.J. Chen, J.T. Wang, X.J. Liu, X. Zhao, W.M. Qiao, D.H. Long, Alkaline carbon nanotubes as effective catalysts for H_2S oxidation, Carbon, 49 (2011) 3773–3780.
[47] F. Zeng, X.F. Liao, Y. Li, Y. He, L. Liao, H. Hui, Preparation of sludge-straw based activated carbon and its adsorption of H_2S, J. Environ. Sci., 37 (2017) 4269–4276.
[48] C. He, A. Giannis, J.Y. Wang, Conversion of sewage sludge to clean solid fuel using hydrothermal carbonization: hydrochar fuel characteristics and combustion behavior, Appl. Energy, 111 (2013) 257–266.
[49] C. Peng, Y.B. Zhai, Y. Zhu, B.B. Xu, T.F. Wang, C.T. Li, G.M. Zeng, Production of char from sewage sludge employing hydrothermal carbonization: char properties, combustion behavior and thermal characteristics, Fuel, 176 (2016) 110–118.
[50] Y.M. Hu, J.C. Jiang, Y.J. Sun, Z.Z. Yang, The thermal effect research during the cellulose pyrolysis process, Renew. Energy Res., 31 (2013) 101–105.
[51] A. Gani, I. Naruse, Effect of cellulose and lignin content on pyrolysis and combustion characteristic for several types, Renew. Energy, 32 (2007) 649–661.
[52] D.Z. Lu, H. Yao, Q.B. Wang, Z.Y. Li, Q.C. Peng, X.W. Liu, M.H. Xu, Effect of cellulose and lignin content on pyrolysis and gasification characteristic for several types of biomass, J. Eng. Thermophys., 29 (2008) 1771–1774.
[53] K.S. Sing, Reporting physisorption data for gas/solid systems with special reference to the determination of surface area and porosity (Recommendations 1984), Pure Appl. Chem., 57 (1985) 603–619.
[54] Z.D. Xie, Study on Preparation and Application of Activated Carbon from Ramie Stalk, Donghua University, Shang Hai, 2012.
[55] L. Gu, P. Zhou, H.P. Yuan, N.W. Zhu, Mechanism and performance of preparation of compositional straw-sludge based activated carbon with different chemical activators, Water Purif. Technol., 32 (2013) 61–66.
[56] Y.B. Xie, W.Y. Zhang, R. Zhang, G. Chen, C.X. Zhang, L.C. Ling, Comparisons of chemical properties and pore structure of carbons activated by KOH and NaOH, Carbon Tech., 2 (2008) 18–23.
[57] R. Azargohar, A.K. Dalai, The direct oxidation of hydrogen sulphide over activated carbons prepared from lignite coal and biochar, Can. J. Chem. Eng., 89 (2011) 844–853.
[58] P. Wang, J.S. Feng, Organic Spectroscopy, National Defend Industry Press, Beijing. 2012.
[59] T.L. Silva, A. Ronix, O. Pezoti, L.S. Souza, P.K.T. Leandro, K.C. Bedin, K.K. Beltrame, A.L. Cazetta, V.C. Almeida, Mesoporous activated carbon from industrial laundry sewage sludge: adsorption studies of reactive dye Remazol Brilliant Blue R, Chem. Eng. J., 303 (2016) 467–476.
[60] M. Angeles Lillo-Ródenas, A. Ros, E. Fuente, M.A. Montes-Morán, M.J. Martin, A. Linares-Solano, Further insights into the activation process of sewage sludge-based precursors by alkaline hydroxides, Chem. Eng. J., 142 (2008) 168–174.
[61] C. Tang, J. Zhua, Z. Lid, R. Zhua, Q. Zhoua, J. Weia, H. Hea, Q. Tao, Surface chemistry and reactivity of SiO_2 polymorphs: a comparative study on a-quartz and a-cristobalite, Appl. Surf. Sci., 355 (2015) 1161–1167.
[62] M. Angeles Lillo-Ródenas, J. Juan-Juan, D. Cazorla-Amoros, A. Linares-Solano, About reactions occurring during chemical activation with hydroxides, Carbon, 42 (2004) 1371–1375.
[63] T. Yang, A.C. Lua, Characteristics of activated carbons prepared from pistachionut shells by potassium hydroxide activation, Microporous Mesoporous Mater., 63 (2003) 113–124.
[64] Y.K. Choi, M.H. Cho, J.S. Kim, Air gasification of dried sewage sludge in a two-stage gasifier. Part 4: Application of additives including Ni-impregnated activated carbon for the production of a tar-free and H_2-rich producer gas with a low NH_3 content, Int. J. Hydrogen Energy., 41 (2016) 1460–1467.